PHYSICAL REVIEW B **74**, 161202(R) (2006)

Deactivation of Li by vacancy clusters in ion-implanted and flash-annealed ZnO

T. Moe Børseth,[1,*] F. Tuomisto,[2] J. S. Christensen,[1] W. Skorupa,[3] E. V. Monakhov,[1] B. G. Svensson,[1] and A. Yu. Kuznetsov[1]
[1]*Department of Physics/Centre for Materials Science and Nanotechnology, University of Oslo, P. O. Box 1126 Blindern, 0318 Oslo, Norway*
[2]*Laboratory of Physics, Helsinki University of Technology, P. O. Box 1100, 02015 TKK, Finland*
[3]*Institute of Ion Beam Physics and Materials Research, Forschungszentrum Rossendorf, P. O. Box 510119, 01314 Dresden, Germany*
(Received 23 August 2006; revised manuscript received 26 September 2006; published 23 October 2006)

Li is present in hydrothermally grown ZnO at high concentrations and is known to compensate both *n*- and *p*-type doping due to its amphoteric nature. However, Li can be manipulated by annealing and ion implantation in ZnO. Fast, 20 ms flash anneals in the 900–1400 °C range result in vacancy cluster formation and, simultaneously, a low-resistive layer in the implanted part of the He- and Li-implanted ZnO. The vacancy clusters, involving 3-4 Zn vacancies, trap and deactivate Li, leaving other in-grown donors to determine the electrical properties. Such clusters are not present in sufficient concentrations after longer (1 h) anneals because of a relatively low dissociation barrier ~2.6±0.3 eV, so ZnO remains compensated until Li diffuses out after 1250 °C anneals.

DOI: 10.1103/PhysRevB.74.161202 PACS number(s): 61.72.Vv, 78.70.Bj, 61.72.Cc, 61.72.Ji

ZnO has great potential as a material for optoelectronic applications.[1,2] Hydrothermally (HT) grown ZnO material is of particular interest, as this growth method is scalable.[3] However, electronic doping issues in ZnO in general, and in HT ZnO in particular, are not fully controlled or understood. For example, the role of lithium needs to be addressed. HT ZnO is synthesized in a solution containing LiOH and is therefore abundant with Li. Lithium's lattice position decides whether it exhibits donor-or acceptorlike character in ZnO; occupying zinc sites (Li_{Zn}) it is an acceptor, occupying interstitial sites (Li_i) it is a donor.[4–6] This amphoteric behavior[7] explains why Li doping produces highly resistive or even semi-insulating[8] material. Interestingly, it has recently been reported that in sputtered thin ZnO films Li may act as a dominating *p*-type dopant.[9] However, the atomistic doping mechanism is not well understood, and the doping efficiency depends strongly on the sputtering and annealing conditions.[9] It is thus important to investigate if and how Li can be (i) stabilized as Li_{Zn} or Li_i, (ii) deactivated or gettered, or (iii) removed from the HT ZnO material. Either scenario would facilitate electronic doping, minimizing compensation by amphoteric Li.

Ion implantation introduces intrinsic defects, and in some cases electronic states associated with the implanted impurity. However, activation of the implanted impurities by annealing results in limited modifications in the conductivity of the highly resistive HT ZnO,[10] presumably because of the amphoteric role of Li. The measurements in Ref. 10 were performed on highly Li-contaminated samples employing conventional anneals at temperatures $\lesssim$1000 °C; these conditions were probably insufficient to remove Li from the samples, but sufficient to promote Li amphoteric behavior. In this work we report on how an extremely fast heat treatment (~20 ms), so called flash annealing, influences the interaction between Li and the implantation-induced defects and how it affects the electrical properties of the ion-implanted ZnO. We have used two types of ions, He^+ and Li^+. The former generates intrinsic defects only, whereas the latter, in addition, alters the Li concentration in the sample. Thus, we are able to distinguish effects caused specifically by Li from effects caused by implantation-induced intrinsic damage. We show that in contrast to conventional anneals, flash anneals of ion implanted ZnO result in the formation of stable clusters of $\gtrsim$3–4 vacancies. Simultaneously, a low-resistive layer is formed in the implanted part of the sample. We suggest that the reduction in resistivity is caused by deactivation of Li by these clusters.

We used highly resistive (~2 kΩ cm), nominally undoped, *n*-type (0001) ZnO, 1×1 cm^2 hydrothermally grown wafers unintentionally contaminated with $\sim5\times10^{17}$ Li/cm^3. The wafers were implanted at room temperature with $^7Li^+$ and $^4He^+$ ions using an energy of 840 and 680 keV and a dose of 2×10^{15} cm^{-2} and 6×10^{15} cm^{-2}, respectively. The projected range (R_p) for both He^+ and Li^+ ions is 1.9 μm, producing similar initial damage profiles in both implants based on TRIM simulations[11] of the vacancy production. After implantation the wafers were cut into $\sim5\times5$ mm^2 pieces and annealed at 500–1250 °C in a conventional furnace or by a flash lamp at 900–1400 °C. As a reference, unimplanted samples were annealed at some selected temperatures. Conventional anneals were performed in an open tube furnace in air whereas for flash anneals,[12] also performed in air, xenon flash lamps were used. The samples annealed by flash at 1200 and 1400 °C were preheated to 500 °C for 5 min immediately prior to the flash anneal.

The Li concentration was measured by depth profiling of $^7Li^+$ ions employing secondary-ion mass spectrometry (SIMS) using a Cameca IMS 7f instrument. A possible correlation between Li redistribution and electrical properties was investigated by a conventional four-point probe sheet resistance measurement setup and a cross-sectional atomic force microscope (AFM) employing scanning spreading resistance microscopy (SSRM) and scanning capacitance microscopy (SCM) modes, using a Veeco D3100 AFM. The SSRM resistance is extracted from the measured current by applying a dc bias between a Ti-Pt-covered silicon tip and the sample so that the signal is proportional to the sample resistivity.[13] SCM was carried out using a similar circuit in dC/dV mode.[13]

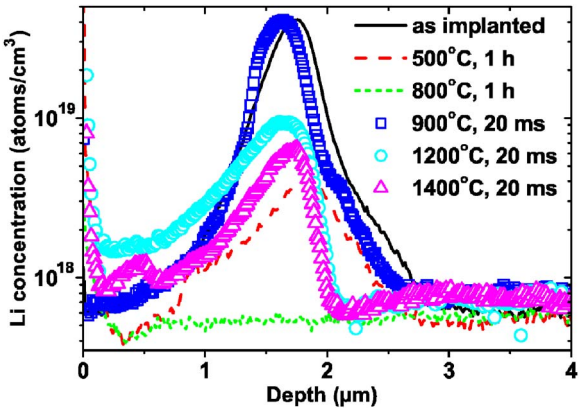

FIG. 1. (Color online) Li concentration versus depth profiles in Li-implanted samples before (solid line) and after conventional (dashed lines) and flash (symbols) annealing as measured by SIMS.

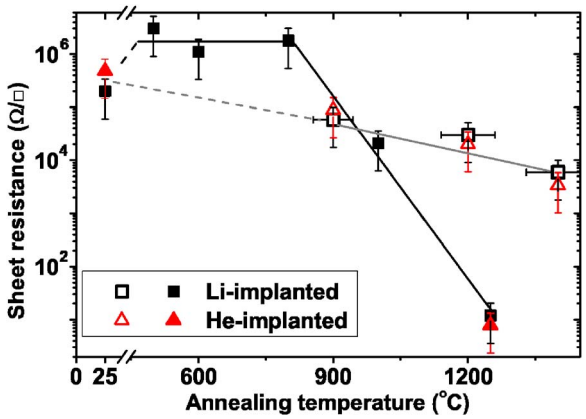

FIG. 2. (Color online) Sheet resistance of Li- and He-ion-implanted ZnO as a function of annealing temperature. Filled symbols are related to conventional (1 h), and open symbols to flash (20 ms) annealed samples. The lines are drawn to guide the eye.

Positron annihilation spectroscopy (PAS) was used to monitor open volume defects in the samples, specifically the behavior of zinc vacancies (V_{Zn}), the dominant irradiation-induced defect detected by PAS in ZnO at room temperature.[14] PAS is based on positron trapping at neutral and negative vacancy defects, which modifies the annihilation characteristics including the Doppler broadening of the 511 keV annihilation line. We characterized the Doppler spectra by conventional line shape parameters representing the fractions of annihilations with low-momentum valence electrons (S) and high-momentum core electrons (W). Typically, open volume defects are seen as an increase (decrease) in the S (W) parameter.[15] The measured S and W parameters are superpositions of S and W parameters corresponding to different positron annihilation states. In the case when only two positron states are observed, the corresponding data points fall on the line connecting the parameters specific to these states in a W-S plot. In this study, the PAS measurements were performed at room temperature using a variable-energy positron beam in the 0–38 keV range. The Doppler broadening of the annihilation radiation was measured using a Ge detector with an energy resolution of 1.24 keV at 511 keV. The S and W parameters are normalized to the S and W parameters of a vapor-phase-grown ZnO sample known to contain a low concentration of defects ($S_{ref}=0.418, W_{ref}=0.0740$).[14]

Figure 1 shows Li concentration versus depth profiles for the Li-implanted samples after conventional and flash anneals. The concentration in the Li-implantation profile decreases with temperature and reaches the original level (5×10^{17} Li/cm^{-3}) already at 800 °C for the conventional anneals. Increasing temperature in the range of 800–1000 °C does not influence the Li concentration considerably. However, after annealing at 1250 °C in a conventional furnace the Li concentration decreases by more than one order of magnitude through the whole sample (not shown). Reference samples show similar behavior upon conventional annealing: unchanged Li concentration at low temperature, and strongly decreased Li concentration in both the unimplanted and a He-implanted sample at 1250 °C. In contrast, flash anneals result in completely different modifications of the Li profiles. First, the Li peak concentration does not go down to the background level. The partial decrease in peak concentration after 1200 and 1400 °C anneals is likely caused by the 500 °C preheating, in accordance with the Li redistribution after a 1 h conventional anneal at 500 °C in Fig. 1. Second, already after 900 °C, the Li peak, while conserving intensity, is shifted slightly toward the surface. This may indicate that the implanted Li atoms decorate the vacancy part of the implantation-induced defect profile, known to be broader and closer to the surface than the implantion profile.[16] In a virgin sample subjected to flash anneals the Li concentration does not change at all. Thus, assuming that the presence of Li causes the high resistivity in HT ZnO, we anticipate a large modification of electrical properties only in the samples subjected to conventional anneals at 1250 °C where the decrease in Li concentration was significant.

Figure 2 summarizes the four-point probe sheet resistance measurements after ion implantation and/or annealing. In accordance with our assumption above, in the 1250 °C conventionally annealed sample the conductivity is significantly improved compared to virgin, as-implanted, or, e.g., 500, 600, or 800 °C annealed samples, clearly indicating the compensating role of Li. Surprisingly, the conductivity improves also in Li-implanted samples subjected to flash-lamp annealing, most prominently at 1400 °C, despite the few times higher Li concentration in the surface layer than that in the virgin sample, Fig. 1. One explanation could be that flash anneals stabilize Li in either its donor or acceptor configuration. However, reference flash anneals of unimplanted ZnO had no effect on the sheet resistance. Similarly to the Li-implanted samples, the sheet resistance also decreased in He-implanted samples after flash annealing, Fig. 2. This indicates that the decrease in sheet resistance is related to radiation damage rather than the nature of the implanted species. It can further be suggested that this decrease is caused by interaction between Li and implantation-induced defects. Indeed, Li remains in high concentration in the flash annealed samples and might be either (A) trapped and passivated in defect complexes so other in-grown donors can dominate, or (B) stabilized as a Li_i donor, or (C) ion implan-

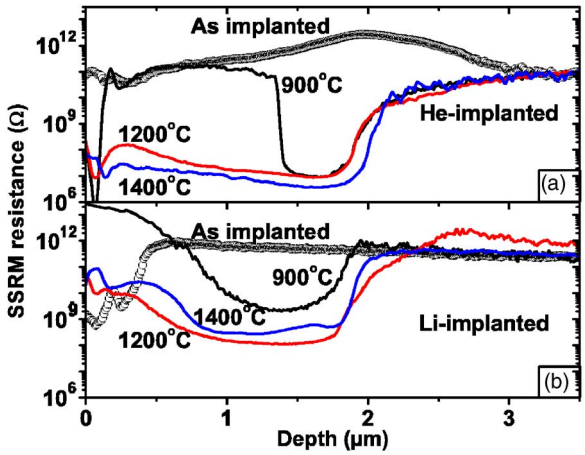

FIG. 3. (Color online) SSRM resistance depth profiles of (a) He- and (b) Li-implanted ZnO for as-implanted and flash-annealed samples.

tation itself might induce enough shallow donors rendering Li-related compensation irrelevant. Already at this point we may exclude stabilization of Li in a Li_{Zn} acceptor state or introduction of predominant acceptors by ion implantation since the material remains *n* type as will be discussed also later.

Figure 3 shows SSRM depth profiles of He- (a) and Li-implanted (b) samples before and after flash anneals. For both the He and Li as-implanted samples, the SSRM resistance is high and similar to the original substrate value (10^{11}–10^{12} Ω). In the He as-implanted sample only, however, the SSRM resistance is not uniform and reaches a maximum at $\sim R_p$, probably because implantation-induced defects trap electrons in this sample, whereas in the Li-implanted samples such traps are more efficiently passivated by Li. Anyhow, conventional anneals at 500–800 °C do not alter the SSRM signal (not shown), which remains similar to that in the as-implanted samples. Further, for the sample conventionally annealed at 1250 °C, the SSRM signal drops substantially to a value of $\sim 10^5$ Ω through the whole wafer depth (not shown). This is in agreement with the four-point probe measurements, and correlates with the decrease in Li content observed by SIMS. Also the SSRM data of the flash-annealed samples are in accordance with the sheet resistance measurements, and after 1200 and 1400 °C treatments, the conductivity improvement takes place mainly in the region containing implantation-induced defects, Fig. 3. In the 900 °C sample, the conductive region is confined to the damage peak and is buried under a highly resistive surface layer, Fig. 3, consistent with the high sheet resistance shown in Fig. 2. The broader conductive region in the Li-implanted than in the He-implanted sample is consistent with the expected broader damage profile considering Li's larger mass. Combining the facts that (i) similar SSRM profiles are observed for Li- and He-ion-implanted samples after flash annealing, Fig. 3 (ii) the conductivity improvement occurs predominantly in the damaged region, (iii) flash annealing of unimplanted material is insufficient to increase the conductivity, (iv) the Li profile is not significantly altered in the flash-annealed samples, Fig. 1, and (v) SCM measurements

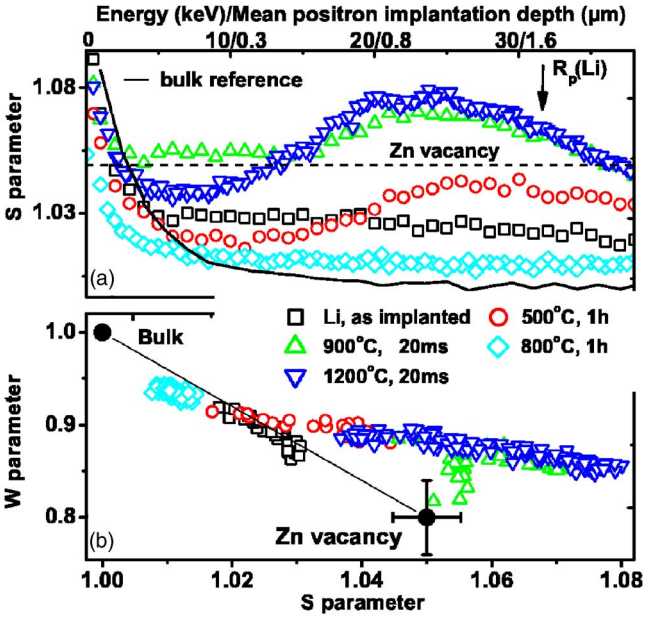

FIG. 4. (Color online) Doppler spectroscopy data for the Li-implanted samples: (a) *S* parameter as function of positron implantation energy; (b) *W*-*S* plot. The *S* and *W* parameters corresponding to positron annihilation at V_{Zn} are from Ref. 14. The dashed line indicates the V_{Zn}-specific *S* parameter.

(not shown) reveal that the samples remain *n* type, we suggest that the conductivity modification in the ion-implanted and flash-annealed HT ZnO is caused by deactivation of Li by radiation defects so other shallow donors may dominate. The possibility of Li being stabilized as Li_i is considered less likely given the similar SSRM profiles in the He- and Li-implanted samples, despite their different Li concentrations. Likewise, the SSRM profiles's flat shape suggest that implantation-induced donor complexes are not the cause of the conductivity increase.

PAS was used to investigate transformations of vacancy-type defects in the implanted layers. Figure 4(a) shows the depth profile of the *S* parameter extracted from typical Doppler broadening spectra for the Li-implanted samples before and after annealing; Fig. 4(b) shows the corresponding *W*-*S* plot. In the as-implanted sample, the *S* parameter increases compared to the reference level indicating an increase in the concentration of open volume defects. After flash annealing at 900 and 1200 °C, the *S* parameter in the implanted region increases substantially to a level well above the value corresponding to saturation trapping by V_{Zn}, Fig. 4(a), indicating vacancy clusters with open volumes larger than that of V_{Zn}. The effect of these clusters is seen also in the *W*-*S* plot [Fig. 4(b)], where the data points for the flash-annealed samples fall away from the line connecting bulk and V_{Zn} annihilation states. Based on the slope of these cluster points in the *W*-*S* plot, we estimate that the vacancy clusters consist of at least 3-4 Zn vacancies (and presumably a similar amount of V_O). This clustering is observed for all three flash-annealing temperatures (the data measured for the 1400 °C flash anneal are omitted in Fig. 4 for clarity as they were essentially identical to the 1200 °C data), but note that for the 900 °C annealed sample, the *S* parameter measured at 5–12 keV

[Fig. 4(a), the near-surface region] coincides with that of V_{Zn}. This region corresponds to the highly resistive surface region observed in Fig. 3(b). Flash annealing at 1200 °C reduces the S parameter in the surface region, implying that V_{Zn} either anneals out, or more likely, takes part in the vacancy clustering in the damage peak region. Similar high S values for the He-implanted samples confirm that the results in Fig. 4 are consistent with the presence of 10^{18}–10^{20} cm^{-3} vacancy clusters and the role of metallic Li—which also could contribute[17]—is insignificant. Combining PAS, SIMS, and electrical measurement results, we conclude that Li in the flash-annealed samples is deactivated by trapping at vacancy clusters. Conventional anneals at 500 °C also induce vacancy clustering (Fig. 4), but to a much smaller extent than flash annealing. These "conventional" clusters do not influence the electrical properties, begin to anneal out at 600 °C (not shown) and disappear completely after conventional annealing at 800 °C, Fig. 4. Similar vacancy clustering has been observed after conventional anneals of nitrogen-implanted ZnO.[18]

In general, cluster generation and growth can take place at rather low temperatures, as long as the vacancy supersaturation level and clustering reaction radii are high, and the diffusion barrier is low. Simultaneously, clusters might start breaking up; the dissociation rate can be approximated by $C=C_0\exp(-E_B/kT)$, where C_0 depends on the lattice vibrational properties, E_B is the cluster dissociation energy, and kT is the thermal energy. Clearly, if E_B is sufficiently high, the clusters are stable once formed regardless of temperature and time. For realistic E_B values, the survival of clusters upon annealing requires a suitable combination of temperature and time. Indeed, in Fig. 4 we observe clusters either for low temperatures and long times (500 °C, 1 h) or high temperatures and short times (e.g., 1200 °C, 20 ms); after 1 h annealing at 800 °C there is no evidence of surviving clusters. The conductive layers formed after 20 ms anneals at 900–1400 °C, Fig. 3, show rather good temperature stability during a 1 h anneal up to ~800 °C, consistent with cluster dissociation becoming efficient at 800 °C, and, consequently, the release of passivated Li. Assuming that C_0 can range from to 10^{10} s^{-1} to the Debye frequency ~10^{13} s^{-1}, and based on relative cluster concentrations in Fig. 4 we estimate the cluster dissociation energy to be ~2.6±0.3 eV for $(V_{Zn})_n$ with $n\sim3$–4.

In summary, we have shown that Li behavior in ZnO can be engineered by appropriate annealing and ion implantation. 20 ms flash anneals in the 900–1400 °C range lead to the formation of vacancy clusters. Simultaneously, a low-resistive layer is formed in the implanted part of the He- and Li-implanted ZnO. The clusters, involving 3-4 Zn vacancies, trap and deactivate Li leaving other in-grown donors determine the material's electrical properties. Such clusters are not present in sufficient concentrations after 1 h furnace anneals because the cluster dissociation barrier is relatively low, ~2.6±0.3 eV, so ZnO remains compensated until Li diffuses out at 1250 °C. The low-resistive layers formed by flash anneals show good temperature stability during 1 h anneals up to ~800 °C when the vacancy clusters dissociate, and the amphoteric behavior of Li reemerges.

We thank M. Rummukainen of the Helsinki University of Technology for technical support with PAS. Financial support from the University of Oslo's FUNMAT program, and from NordForsk through the NOCDAD collaboration, is gratefully acknowledged.

*Electronic address: t.m.borseth@fys.uio.no

[1] Y. R. Ryu, T. S. Lee, J. A. Lubguban, H. W. White, Y. S. Park, and C. J. Youn, Appl. Phys. Lett. **87**, 153504 (2005).

[2] A. Tsukazaki, M. Kubota, A. Ohtomo, T. Onuma, K. Ohtani, H. Ohno, S. F. Chichibu, and M. Kawasaki, Jpn. J. Appl. Phys., Part 2 **44**, L643 (2005).

[3] K. Maeda, M. Sato, I. Niikura, and T. Fukuda, Semicond. Sci. Technol. **20**, S49 (2005).

[4] J. J. Lander, J. Phys. Chem. Solids **15**, 324 (1960).

[5] C. H. Park, S. B. Zhang, and S. H. Wei, Phys. Rev. B **66**, 073202 (2002).

[6] E. C. Lee and K. J. Chang, Phys. Rev. B **70**, 115210 (2004).

[7] M. G. Wardle, J. P. Goss, and P. R. Briddon, Phys. Rev. B **71**, 155205 (2005).

[8] N. Y. Garces, L. Wang, N. C. Giles, L. E. Halliburton, D. C. Look, and D. C. Reynolds, J. Electron. Mater. **32**, 766 (2003).

[9] Y. J. Zeng, Z. Z. Ye, W. Z. Xu, D. Y. Li, J. G. Lu, L. P. Zhu, and B. H. Zhao, Appl. Phys. Lett. **88**, 062107 (2006).

[10] T. Moe Børseth, J. S. Christensen, K. Maknys, A. Hallén, B. G. Svensson, and A. Y. Kuznetsov, Superlattices Microstruct. **38**, 464 (2005).

[11] J. F. Ziegler, Nucl. Instrum. Methods Phys. Res. B **219**, 1027 (2004).

[12] W. Skorupa, R. A. Yankov, W. Anwand, M. Voelskow, T. Gebel, D. F. Downey, and E. A. Arevalo, Mater. Sci. Eng., B **114–115**, 358 (2004).

[13] M. Stangioni, M. Ciappa, and W. Fichtner, Microelectron. Reliab. **45**, 1532 (2005).

[14] F. Tuomisto, V. Ranki, K. Saarinen, and D. C. Look, Phys. Rev. Lett. **91**, 205502 (2003).

[15] K. Saarinen, P. Hautojärvi, and C. Corbel, in *Identification of Defects in Semiconductors*, edited by M. Stavola (Academic Press, New York, 1998), p. 209.

[16] S. Coffa, V. Privitera, F. Priolo, S. Libertino, and G. Mannino, J. Appl. Phys. **81**, 1639 (1997).

[17] M. A. van Huis, A. van Veen, H. Schut, C. V. Falub, S. W. H. Eijt, P. E. Mijnarends, and J. Kuriploch, Phys. Rev. B **65**, 085416 (2002).

[18] Z. Q. Chen, M. Maekawa, A. Kawasuso, R. Suzuki, and T. Ohdaira, Appl. Phys. Lett. **87**, 091910 (2005).